

Designing the measurement cell of a swept-field differential aspiration condenser

A.A. Solis and E. Sacristán

Departamento de Ingeniería Eléctrica, Universidad Autónoma Metropolitana, Michoacán y Purísima, Col. Vicentina, Iztapalapa, México D.F., 09340, México.

Recibido el 25 de noviembre de 2005; aceptado el 22 de marzo de 2006

We present the description of a small-size and low-cost sensor based on the aspiration method that can be used as an ion-mobility spectrometer: the planar swept-field first-order differential aspiration condenser. A mathematical model for the measurement cell of the condenser has been developed, and in this paper a design strategy based on the model is described. A measurement cell has been constructed following this strategy and was used in a prototype aspiration condenser device. Some collector-plate ion-current curves have been measured for gas samples with several different anesthetic gases in different concentrations in order to evaluate the model and the design of the measurement cell. The inverse transform via the truncated singular value decomposition (TSVD) has been applied to the data to obtain ion-mobility spectra. The results suggest that, although the model simplifies the actual physical behavior of the ions, thereby causing some inconsistencies in the mobility spectra, it is still useful in the aspiration condenser's design process. The proposed device is an attractive small-size, cost-effective alternative for ion-mobility gas analysis applications.

Keywords: Aspiration condenser; gas monitoring; ionization; ionic mobility; spectrometry; Tammets transform.

Presentamos la descripción de un nuevo sensor basado en el método de aspiración, pequeño y de bajo costo, que puede ser utilizado como un espectrómetro de movilidad iónica: el condensador de aspiración plano de primer orden con barrido de campo. Se ha desarrollado un modelo matemático de la celda de medición del sensor, y basado en éste se describe en este artículo un método estructurado para su diseño. Aplicando el método propuesto se ha construido una nueva celda de medición y se ha empleado en un condensador de aspiración prototipo. Se presentan a modo de evaluación del modelo y del diseño algunos espectros de movilidad iónica obtenidos por medio de la transformación inversa por truncamiento de la descomposición en valores singulares (TSVD) del modelo matemático, aplicada a las curvas de voltaje obtenidas mediante el sensor para una mezcla gaseosa con diferentes concentraciones de agentes anestésicos. Los resultados sugieren que, aunque el modelo simplifica el comportamiento físico de los iones, causando algunas inconsistencias en el espectro de movilidad, es de una gran utilidad en el proceso de diseño de un condensador. El dispositivo propuesto se perfila como una alternativa atractiva de bajo costo y tamaño pequeño para aplicaciones de análisis de gases por movilidad iónica.

Descriptores: Condensador de aspiración; monitoreo de gases; ionización; movilidad iónica; espectrometría; transformada de Tammets.

PACS: 02.30.Rz; 02.30.Zz; 07.81.+a; 51.50.+v

1. Introduction

Current ion-mobility spectrometers are precision instruments for the detection of trace chemicals in the air [1-4] and are nowadays well established as useful analytical chemistry tools that, nonetheless, are relatively complex, and whose size and cost have limited their field applications. Many efforts have been made towards reducing these limitations [5-7], and recent advances have made progress in this area [22-28], resulting in instruments of reduced size and cost. However, a simpler method for ion-mobility analysis has existed since the end of the 19th century [8,9] and has been used in a variety of device configurations and applications [10-14]: *the aspiration method*. This technique requires a much simpler and inexpensive instrument design (with the simplicity of a smoke detector), though it has some inherent limitations with regard to measurement: it has poor ion-mobility resolution, a weighted integral measurement of ion mobilities in the sample, and is normally tuned to one or more fixed voltage points or channels, thereby precluding the obtaining of a true ion-mobility spectrum. Our research goal is to benefit from the advantage of the small size and low cost of a simple aspiration condenser [10,33] in finding a solution for the resolution problem and providing ion-mobility spectra, in

order to examine different possible applications, such as the development of an inexpensive anesthesia monitor for clinical applications. Sacristán and Solis [16,17] have previously analyzed the theory of operation of a swept-field differential aspiration condenser of the first order, and in this paper the authors describe a design procedure for the measurement cell of this device based on the mathematical model they previously proposed. This procedure is then followed in the construction of a new measurement cell, which is in turn tested by obtaining the ion-mobility spectra of some gas mixtures that can be expected in the application of anesthesia.

2. Background

2.1. Ion-Mobility Spectrometry (IMS)

Originally known as plasma chromatography, IMS deals with the principles, practice and instrumentation through which gas-phase chemicals are characterized by the mobility of their ionized molecules, and it was introduced in the late 1960's as a method for detecting trace concentrations of organic compounds in air and other gases [2,3]. Different techniques based on this principle are available, but in a traditional drift-tube ion-mobility spectrometer, trace chemicals

in a carrier gas sample are introduced into the reaction region where neutral molecules are ionized by a radioactive source. Long-lived, low-energy, relatively stable ion clusters are formed through electron and proton transfer reactions [2]. Product-ions rarely dissociate or fragment because the energies involved in ionization at atmospheric pressures are usually weak. Another consequence of this fact is that only a few dominant product-ion species are created, and these are structurally related to the original neutral molecules.

The product-ions are then injected into the drift region where the ion-mobility discrimination is performed. An electric field, parallel to the axis of the drift tube, effectively separates the ions by imparting a constant mean drift velocity v_d to each particle, proportional to their ion-mobility K and the intensity of the field E :

$$v_d = KE. \quad (1)$$

The ions separated in this manner travel the length of the drift tube and are captured by a detector at the other end, where an ion-mobility spectrum can be recorded as a graph of the ionic current generated by the colliding ions against the time of impact for each species.

The advantages of this technique over other well-established technologies such as mass spectrometry or gas chromatography/mass spectrometry are in general practical considerations of energy consumption, size, weight and price.

2.2. The Aspiration Method

The aspiration method applied to the field of ion-mobility spectrometry represents a lower-cost, smaller-size alternative to traditional drift-tube IMS devices. In this technique the sampled gas is introduced directly to the device without a carrier gas, it is ionized, and the resulting product-ions are delivered to a measurement cell with one or several electrode pairs arranged in a condenser-like array, creating an electric field perpendicular to the gas flow. Puumalainen and Paakkanen [10,21,33,34] have developed a very low-cost sensor using this method, and their measurement-cell has several condenser-like pairs of plates that can be built rather inexpensively using printed circuit-board (PCB) technology. This device has been successfully employed in military and industrial applications and is commercially available as the multi-channel IMCell™ ionization and measurement cell in instruments built by Environics Oy, a company from Mikkeli, Finland (www.environics.fi).

The main advantages of this method over traditional drift-tube IMS devices are speed and time-independence, being able to measure almost continuously because the cell has a very fast recovery time [35]. Furthermore, detection of both positive and negative ions at the same time is possible, no carrier or drift gas are required, and the cell is tolerant to great quantities of sampled gas [21,32,36]. In the particular case of clinical anesthesia monitoring applications, for example, this means that no additional servo-controlled gas dilut-

ing system is required [29], thereby lowering the cost of such instruments.

On the other hand, aspiration condensers share some limitations with respect to conventional IMS devices, such as low-resolution, limited dynamic-range and concentration dependence [33]. Also, the device we have discussed above only samples a point of an ion-current spectrum at every detection-plate or channel, and does not provide an ion-mobility spectrum.

Sacristán and Solis [16,17] have described a simplified theoretical analysis of a swept-field differential, first-order aspiration condenser that evolved from the Puumalainen design. A diagram of this sensor is shown in Fig. 1. The measurement cell of the device (Fig. 2) mainly consists of three electrodes or plates: frontal and collector plates, and a reference plate. Neutral molecules in the gas to be analyzed flow into a chamber, where they are ionized by a radioactive element (in this case, ^{241}Am emitting alpha particles with 5.92 MeV is used). Ionized molecules then form clusters and/or are involved in proton- or electron-transfer reactions

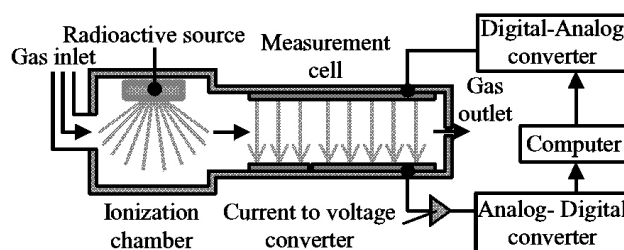


FIGURE 1. Planar differential swept-field aspiration condenser. A gas sample is ionized using a radioactive source, ^{241}Am . Ions then react with other ionized or neutral molecules resulting in clusters called product-ions, which then flow into the measurement cell of the condenser, where an electric field, parallel to the flow, is generated between polarized electrodes. Depending on the direction and intensity of this field, ions of a given polarity are deflected towards the measuring electrodes, producing an ion-current signal which is detected by a computer using only the collector plate. Sweeping the voltage applied to the reference plate, an ionic-current spectrum can be obtained.

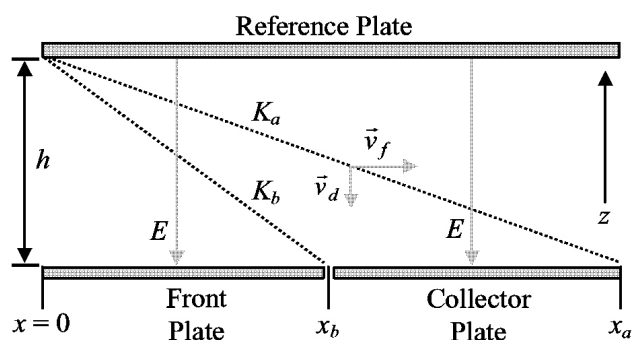


FIGURE 2. Measurement cell. An ion flowing through the cell is deflected by an electric field E . The frontal electrode captures all ions having mobility $K > K_b$ and the collector plate captures all ions with mobility $K > K_a$, except those captured by the frontal plate. Hence the term “differential”.

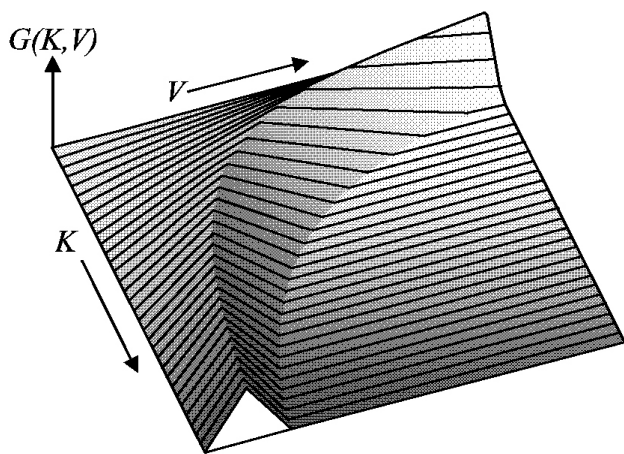


FIGURE 3. 3D representation of the G-function or capture efficiency of the collector plate of a differential aspiration condenser for a given range of voltages and ion-mobilities, the morphology of which depends on the geometry of the measurement cell if the flow-rate is constant. A hyperbolic relationship exists between voltage and mobility.

with other charged or neutral molecules, forming products prior to flowing into the measurement cell. In particular, volatile halogenated anesthetics (VHAs) tend to form negative ions [1,2]. A previous application of traditional IMS to the analysis of these chemicals [29] shows that VHAs go through ionization reactions where the halogen atoms in the gas tend to capture an electron and dissociate from the parent molecule, and then associate with other neutral or ionized molecules through charge-transfer interactions, the size of the product-ion cluster being dependent on the concentration of anesthetic agent.

Product-ions then flow into the measurement cell passing through the electric field created between the reference and front/collector electrodes, arrayed in a condenser-like geometry. Ions of a given polarity are deflected toward the measuring electrodes by field E perpendicular to the flow, generated by applying voltage to the reference plate (the measuring electrodes are grounded). In contrast to the Puumalainen device, however, the signal is detected using only one of the electrodes, the collector plate, but the reference plate voltage is swept to produce an ion-current spectrum.

In order to control the average ion-trajectory to separate the ions by their mobility, a laminar flow must be maintained in the measurement cell. The laminar flow profile is parabolic, with maximum flow at the center and minimum where it meets the cell's walls; but to simplify the theoretical model we only consider the average ion trajectory. An ion-current spectrum $I(V)$ is measured by sweeping the reference voltage, and this curve is a transformed function of the ion-mobility spectrum of the gas. This mathematical transform, described by Tammet [18], is defined as

$$I(V) = \int f G(V, K, f) D(K) dK, \tag{2}$$

where the kernel $G(V, K, f)$ is the Green's function (or *G-function*) of the collector plate and is a function of the deflec-

tion voltage V , the ion-mobility K , and the flow rate f of the gas through the cell. The ion-mobility distribution $D(K)$ in the ionized gas sample is equal to the specific charge density of all ions with mobility K . The front plate captures all ions with mobility $K > K_b$, and the collector plate captures all ions with mobility $K > K_a$, except ions already captured by the front electrode, and this is why this device is classified as "differential". K_a and K_b represent limiting mobilities for ions to be captured by the measuring electrodes, as seen in Fig. 2.

The form of the G-function describes the ion capture efficiency of the collector plate, and for the same range of voltages in V and mobilities in K it depends only on the flow rate of the gas sample f and the geometry of the measurement cell (distance from the beginning of the cell to the end of the front plate x_b , distance to the end of the collector plate x_a , and cross-sectional area of the channel $s = wh$, where h is the distance between reference and measurement plates and w is the width of the electrodes). Considering the flow rate to be constant, we can define the quantities A and B as

$$A = \frac{h^2 v_f}{x_a}, B = \frac{h^2 v_f}{x_b}, v_f = \frac{1000f}{60wh}, \tag{3}$$

where v_f is the velocity of the flowing gas sample.

The G-function can be written as

$$G(K, V) = \begin{cases} KVA^{-1} - KVB^{-1} & \text{if } A \geq KV \geq 0 \\ 1 - KVB^{-1} & \text{if } B \geq KV \geq A \\ 0 & \text{if } KV \geq B. \end{cases} \tag{4}$$

This equation defines two hyperbolic limits between three different areas in Fig. 3. The first area is defined between the axes and the first hyperbola $KV = A$ and has a positive slope. The second area is defined between the first area and the second hyperbola $KV = B$ and has a negative slope. The final area is between the second hyperbola and infinity and has a zero slope. From a discrete perspective, the G-function can be perceived as a family of triangles.

The optimum capture efficiency, that is, the maximum value of the G-function, is reached when $KV=A$. From Eqs. (3) and (4),

$$G_{max} = 1 - \frac{A}{B} = 1 - \frac{x_b}{x_a}. \tag{5}$$

Since $x_b < x_a$ and both are positive values, G_{max} is always positive and less than one, and depends only on the size of the measuring electrodes.

In order to use the aspiration condenser as an ion-mobility spectrometer, an ion-mobility density function $D(K)$ must be extracted from the ion-current spectrum $I(V)$ using Eq. (2). In practical situations, $I(V)$ is measured in a digital fashion using an analog-to-digital converter, and we must define a discrete version of the Tammet transform. If the flow rate is constant, the discrete direct Tammet transform can be written as

$$\mathbf{i} = f\mathbf{G}\mathbf{d}, \tag{6}$$

and if \mathbf{G} is a square, non-singular array, then the discrete inverse Tammet transform can be defined as

$$\mathbf{f} \mathbf{d} = \mathbf{G}^{-1} \mathbf{i}, \tag{7}$$

where \mathbf{i} is a vector containing the elements of the characteristic curve $I(v_j)$

$$\mathbf{i} = [I(v_1) \quad I(v_2) \quad \dots \quad I(v_n)]^T, \tag{8}$$

\mathbf{d} is a vector containing the elements of the ion-mobility density function $D(k_i)$

$$\mathbf{d} = [D(k_1) \quad D(k_2) \quad \dots \quad D(k_n)]^T, \tag{9}$$

and \mathbf{G} is a square, non-singular array containing elements $\Delta G(k_i, k_j)$, where $\Delta k_i = k_i - k_{i-1}$

$$\begin{bmatrix} \Delta k_1 G(k_1, v_1) & \Delta k_1 G(k_1, v_2) & \dots & \Delta k_1 G(k_1, v_n) \\ \Delta k_2 G(k_2, v_1) & \Delta k_2 G(k_2, v_2) & \dots & \Delta k_2 G(k_2, v_n) \\ \vdots & \vdots & \ddots & \vdots \\ \Delta k_n G(k_n, v_1) & \Delta k_n G(k_n, v_2) & \dots & \Delta k_n G(k_n, v_n) \end{bmatrix}, \tag{10}$$

and where

$$\forall i = 0 \rightarrow n : k_i = A/v_i \quad \text{y} \quad v_i > 0. \tag{11}$$

The hyperbolic relationship between the voltage and mobility domains is preserved by (11) in order to find a unique solution. If this requirement is not met, since Eq. (2) is an ill-conditioned Fredholm integral equation, regularization [20] or pseudo-inverse methods can be used to find an approximation to the solution.

The discrete G-function consists of a series of hyperbolic impulse-walls given by

$$KV = A \left(\frac{x_b}{x_a} \right)^l \quad \text{where} \quad l = 0, 1, 2, \dots, \infty. \tag{12}$$

3. Methodology

3.1. Design parameters

A and B are important design parameters. As discussed above, the G-function has three regions defined by KV : $0-A$ (positive slope), $A-B$ (negative slope) and $B-\infty$ (zero slope). Other design variables (Fig. 1) are x_b (size of frontal plate), x_a (size of frontal + collector plates), h (cell height), w (cell width) and f (sample gas flow-rate). Modifying these parameters also affects

- The maximum capturing efficiency (G_{max})
- The slope of region $0-A$
- The slope of region $A-B$
- Gas-flow laminarity
- The required gas flow-rate (f)
- The number of hyperbolic impulse-walls in the inverse G-function (which directly affect error in the presence of noise)

- The range and resolution required for the mobility domain

G_{max} is defined by Eq. (5). When $x_b \cdot x_a^{-1}$ tends to zero, then the maximum value of G_{max} tends to unity. Then, if $x_a \gg x_b$, the capture efficiency will be maximum and the collector plate will be much larger than the front plate. There is a limit here, however, because we want the condenser to be as small as possible. The slope of region $0-A$ is directly proportional to h and inversely proportional to x_a and determines the form of the inverse G-function, which is composed of a series of hyperbolic impulse-walls, described by (12). The first wall is situated at $KV = A$, and the rest lie between this and zero. These walls introduce significant error into the inverse transform when noise is present; hence it is desirable to eliminate as many as possible. This can be accomplished by changing the ratio $x_b \cdot x_a^{-1}$.

The slope of region $A-B$ is directly proportional to h and inversely proportional to w and x_b . Together with region $0-A$, it determines the form of the *direct Tammet transform*.

The Reynolds number

$$R_D = \frac{v_f h}{\nu} = \left(\frac{1000 f}{60 w v} \right) \tag{13}$$

gives an indication of gas flow laminarity, where ν is the viscosity of the sample gas and v_f is its flow velocity. Lower R_D values indicate laminar flow, while higher values mean that the flow becomes increasingly turbulent. Laminarity may then be achieved by incrementing w or lowering the flow rate.

For a given mobility interval, the appropriate voltage interval can be found using $KV = A$, thereby assuring that an inverse Tammet solution exists. Although a solution can be found even when this condition is not met using regularization [20] or pseudo-inverse tools, it is desirable to design the measurement cell based on the existence of a traditional solution, since this guarantees that no loss of information exists in the desired range. On the other hand, it is desirable for the whole voltage range to be sampled by the A/D converter, and the value of A must be determined using $K_{max} V_{min}$ or $K_{min} V_{max}$. In general, the second relationship is adequate, because the mobility range that we want the device to sample can be known a priori and the voltage range of the A/D converter is fixed.

Finally, as mentioned, above the flow rate affects laminarity and the values of A and B , and therefore its effect on the slopes of the G-function must also be considered.

3.2. Practical measurement-cell design

We first define the desired mobility interval $[K_{min}, K_{max}]$ and the maximum sample-gas flow rate f_{max} . The maximum deflection voltage V_{max} is known; thus we define

$$A = K_{min} V_{max}. \tag{14}$$

TABLE I. Design specs for the proposed cell design

V_{min}	1.2 V
V_{max}	10 V
K_{min}	$0.18 \text{ cm}^2(\text{Vs})^{-1}$
K_{max}	$1.5 \text{ cm}^2(\text{Vs})^{-1}$
x_b	0.2315 cm
x_a	2.3148 cm
w	0.32 cm
h	0.04 cm
f_{max}	2 lpm

Using this relationship, we can determine the minimum voltage needed to sweep the chosen mobility range

$$V_{min} = \frac{A}{K_{max}}, \quad (15)$$

and then we can set a good Reynolds number for Eq. (13) as follows. Viscosity is a physical parameter that changes from fluid to fluid; therefore, we will approximate the sample-gas viscosity for general applications by that of air

$$\nu_{air} = 0.1487603306 \frac{\text{cm}^2}{\text{s}} \quad \text{a } 20^\circ\text{C y } 1 \text{ atm.} \quad (16)$$

The Reynolds criterion indicates that flow is laminar for R_D values under 1500, transitional between 1500 and 4000, and turbulent above that. A good value for the Reynolds number is $R_D = 700$. Now we can find a value for the width of the cell that guarantees laminar flow

$$w = \frac{1000f_{max}}{60R_D\nu}. \quad (17)$$

With this information, we can now determine the length of each measurement electrode. First, x_a can be determined if we specify the height of the cell h . In our fabrication process, this parameter is known as it is given by Teflon™ spacers. So,

$$x_a = \frac{1000f_{max}h}{60Aw}. \quad (18)$$

G_{max} must be as close to unity as possible, because the maximum ion-current (usually in the μA range) depends on this value. Also, together with x_a and x_b , it determines the position of the impulse-walls of the inverse-function (12), and it is desirable for these to be positioned outside of the region of interest. For this we need

$$K_{min}V_{min} > A\frac{x_b}{x_a} \quad \text{or} \quad K_{min}V_{min} > \frac{A^2}{B}. \quad (19)$$

From this relationship,

$$B_{min} = \frac{A^2}{K_{min}V_{min}} \quad (20)$$

and so

$$x_{b_{max}} = \frac{1000f_{max}h}{60B_{min}w} \quad (21)$$

This is an upper bound for x_b . Using Eqs. (18), (20) and (21) with Eq. (5), we can determine a minimum value for G_{max} :

$$\min G_{max} = 1 - \frac{K_{min}V_{min}}{A}. \quad (22)$$

A higher gain than this is limited by the manufacturing process and the physical behavior of ions and the electric field. We do not want x_b to be *too small*, so $\min G_{max}$ will be enough. Nonetheless, this value can be made a little bit larger to compensate for numerical rounding and manufacturing imprecision. If G_{max} is lower than $\min G_{max}$, some capturing efficiency and noise immunity will be lost.

4. Results

Using the proposed design method, we have determined the parameters for a new measurement-cell with a maximum deflection of 10 V and a mobility range of $[0.18, 1.5] \text{ cm}^2 \cdot (\text{V} \cdot \text{s})^{-1}$, to be used with a 0.04 cm Teflon™ spacer, and considering a maximum sample-gas flow rate of 2 lpm. The value of $\min G_{max}$ is then determined to be 0.88, which in turn gives a value for x_b of 0.2778 cm. G_{max} is then chosen by rounding $\min G_{max}$ to 0.9, which implies that $B = 10A$.

Using these design specifications, a measurement-cell was built and incorporated into an aspiration condenser, and several experiments were conducted with a sample-gas mixture of 80% O₂ and 20% CO₂ at 1 liter per minute, to which several halogenated anesthetic agents (halothane, isoflurane and sevoflurane) were added in different concentrations. We chose these combinations only for purposes of illustration, but our final research is aimed at studying clinical anesthesia mixtures from the exhaled air of a patient. Experiments involving respiratory gases (O₂, N₂ and CO₂), VHAs (desflurane, enflurane, halothane, isoflurane and sevoflurane) and the auxiliary anesthetic gas N₂O are underway.

The chosen gas mixtures were made to flow through the device at 1 lpm and the response was measured at the collector plate. Figure 4 shows the results for a mixture with isoflurane at two different concentrations: 0.5 and 3.5%. Figure 6 shows comparative results for mixtures having halothane and isoflurane at 3.5%. By applying the theoretical model with truncated singular value decomposition (TSVD) regularization [20] with 12 components we were able to obtain an ion-mobility spectrum for each of these curves. The spectra were generated for a larger mobility range in order to determine whether the limits chosen for the designed cell were appropriate, since only previous information from experiments with a traditional IMS device were available [19] to predict it. Ion-mobility spectra for the data of Fig. 4 is shown in Fig. 5. Spectra for the data of Fig. 6 are shown in Fig. 7.

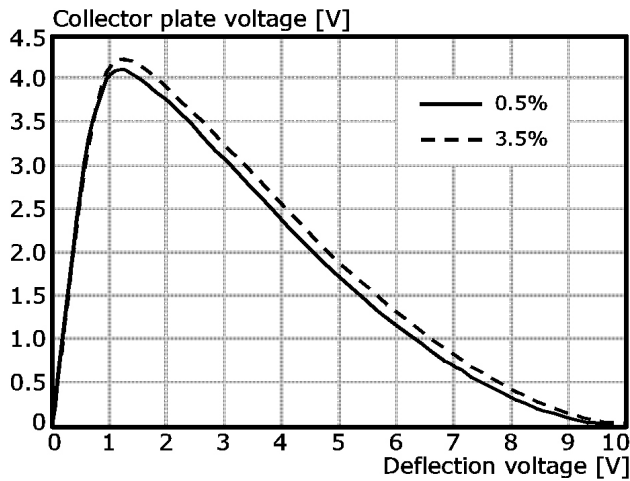


FIGURE 4. Collector ion-current generated by the collision of negative product-ions in an 80% O₂ / 20% CO₂ sample gas with concentrations of 0.5 and 3.5% isoflurane.

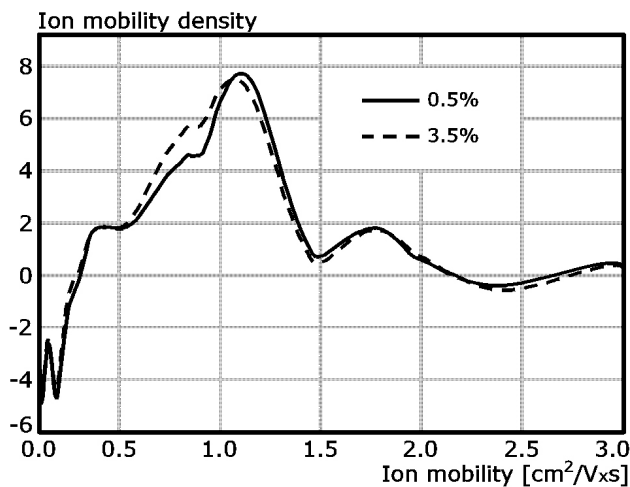


FIGURE 5. Ion-mobility distribution of negative product-ions in an 80% O₂ / 20% CO₂ sample gas with concentrations of 0.5 and 3.5% isoflurane.

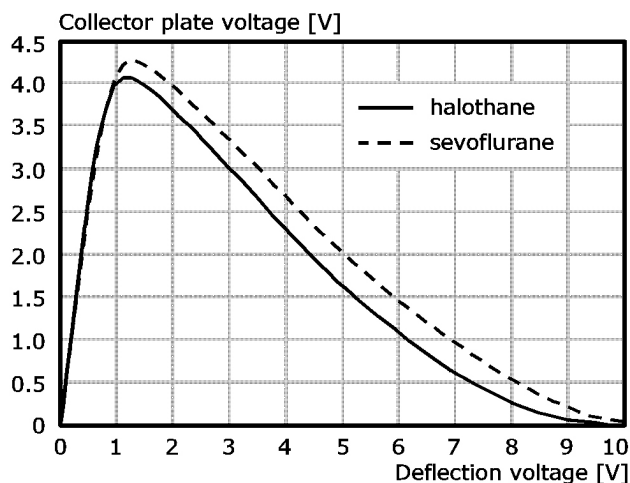


FIGURE 6. Collector ion-current generated by the collision of negative product-ions in an 80% O₂ / 20% CO₂ sample gas with an anesthetic agent concentration of 3.5% (halothane vs. sevoflurane).

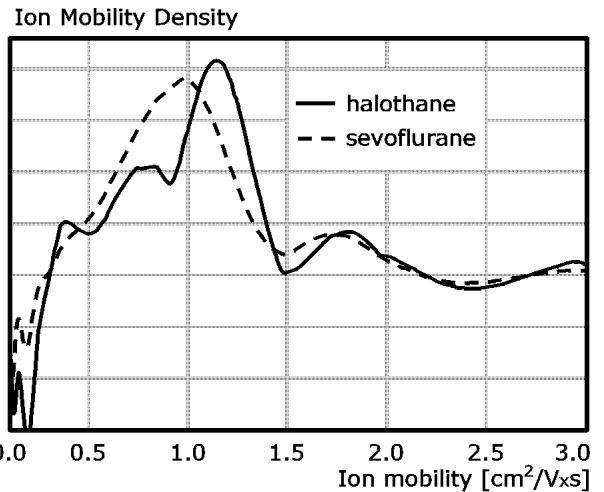


FIGURE 7. Ion-mobility distribution of negative product-ions in an 80% O₂ / 20% CO₂ sample gas with an anesthetic agent concentration of 3.5% (halothane vs. sevoflurane).

5. Discussion

Ion-current curves (Figs. 4 and 6) bear a similar morphology, but slight differences might help for identification purposes. Mainly amplitude differences are seen in Fig. 4, but there are slight morphological differences too. Figure 6 shows mainly morphological differences. Similarities are to be expected in all cases due to the smoothing action of the integral Tammet equation (2).

On the other hand, mobility spectra (Figs. 5 and 7) show the largest differences for different mixtures. Figure 5 shows that at higher concentrations product-ions tend to have less mobility, a fact that is in agreement with traditional IMS experiments [29]. Figure 7 shows that different anesthetic agents have differently shaped spectra. These effects allow easier agent identification than using only ion-current spectra.

Pertaining to the mobility range, we can see that the main ion species are within the range specified in the design process, from 0.13 to 1.5 cm²/V·s, but that some less important species lie outside of it. This is due to the fact that higher-mobility species really do exist, but there are also some oscillations generated by the regularization process. Also, it must be kept in mind that the simplified model does not account for second-order effects and complex ion trajectories, and hence minor errors are expected when performing the inverse transform. This error is visible mostly at lower mobilities, where slow ions are obviously not correctly modelled and non-physical negative quantities are registered.

6. Conclusion

In this paper, a simple low-cost alternative method for chemical gas analysis by ion-mobility spectrometry based on the aspiration method is presented and illustrated with an application in the field of anesthesia-monitoring. A design

methodology for the construction of a measurement-cell for this device has been proposed and a sample cell has been designed and constructed following these ideas. Results show that the device works fairly appropriately, but that the theoretical model has some shortcomings when an exact ion-mobility spectrum is needed. The spectra obtained using this method, however, show what seems to be a good approximation to the real distribution of product-ions in the sampled gas, and the model can definitively be used as a first approx-

imation to the identification and quantification of gas mixtures, if these shortcomings are kept in mind.

In the future, second-order effects, as well as a more accurate description of ion-trajectories in the measurement cell, among other things, must be incorporated into the theoretical model. The use of the device for clinical anesthesia monitoring, one of many possible applications, is also currently being developed.

1. H.H. Hill, W.F. Siems, R.H. St Louis, and D.G. McMinn, *An. Chem.* **62** (1990) 1201A.
2. G.A. Eiceman and Z. Karpas, *Ion-Mobility Spectrometry* (CRC Press Inc., Boca Raton FL, 1994).
3. Karasek and W. Francis, *An. Chemistry* **46** (1974) 710.
4. J. Brokenshire and N. Pay, "Ion-Mobility Spectrometry: A Promising Technology For Environmental Measurement" (International Laboratory, 1989).
5. NASA, "Field-Domain Ion-Mobility Spectrometry", *NASA Technical Support Package*, KSC-11465.
6. G.A. Eiceman "Adv. in Ion-Mobility Spectrometry: 1980-1990" (Critical Reviews in Analytical Chemistry, CRC Press Inc. 1991) p. 17.
7. G. Thekkadath, "Simple Compact Ion-Mobility Spectrometer Having a Focusing Electrode Which Defines a Non-Uniform Field for the Drift Region", *U.S. Pat. #5,189,301* (1993).
8. W. Giese, *Ann. Physik* **17** (1882) 1, 236, 519.
9. J.J. Thomson and E. Rutherford, *Philos. Magazine* **72** (1896) 392.
10. P. Puumalainen, *U.S. Pat. #5,047,723* (1991).
11. A. Jenkins, *U.S. Pat #4,831,254* (1989).
12. Y. Sugiyama and Y. Sagamihara, *U.S. Pat. 4,704,536* (1987)
13. D.A. Blyth, *U.S. Pat. #4,368,388* (1983).
14. S.L. Allman, C. Chen, and F. Chen, *U.S. Pat. #5,184,015* (1993).
15. E. Sacristán, *U.S. Pat. # 5,455,417* (1995).
16. E. Sacristán and A. Solis, *IEEE Trans. on Instrumentation and Measurement* **47** (1998) 769.
17. A. Solis, "Condensador de Aspiración con Barrido de Campo para el Monitoreo de Gases Anestésicos", *UAM Iztapalapa, Tesis de Maestría* (1999).
18. H.F. Tammet, "The Aspiration Method for the Determination of Atmospheric-Ion Spectra", *Scientific Notes of Tartu State University, Issue 195, Transactions on Air Ionization and Electroaerosols, Tartu Estonia (1967) Translated from Russian by the Israel Program for Scientific Translations, Jerusalem (1970).*
19. E. Sacristán, "Ion-Mobility Method for Inhalation Anesthesia Monitoring", *Ph.D. Dissertation, Worcester Polytechnic Institute, Worcester, MA* (1993).
20. P.C. Hansen, *BIT* **27** (1987) 534.
21. K. Tuovinen, H. Paakkanen, O. Haanninen, and J. Ruuskanen, *AIHA Journal* **62** (2001) 80.
22. A.P. Snyder *et al.*, "Portable, Handheld Instrumentation: Gas Chromatography / Ion-Mobility Spectrometer", *Proceedings of the International Symposium on Field Screening Methods for Hazardous Waste and Toxic Chemicals, Las Vegas, NV* **62** (1993) 831.
23. H.H. Hill, "Recent Developments in Ion-Mobility Spectrometry as a Chemical Sensor", *NATO-Russia Workshop on Ecological Risks Associated with the Destruction of Chemical Weapons, Luneburg, Germany* (Oct 2003).
24. H.H. Hill, "Ion-Mobility Comes of Age", *Pittsburg Conference on Analytical Chemistry and Applied Spectroscopy* (Mar 2003).
25. J. Baker *et al.*, "A Miniaturized Ion-Mobility Spectrometer (IMS) Sensor for Wireless Operation", *FAME (Frontiers in Assessment Methods for the Environment) Symposium, Minneapolis, MN* (Aug 2003).
26. R.E. Ewing, G.J. Ewing, D.A. Atkinson, and G.A. Eiceman, *Talanta* **54** (2001) 515.
27. G.A. Eiceman, E.G. Nazarov, J.A. Stone, *Analytica Chimica Acta* **493** (2003) 185.
28. G.A. Eiceman, E.G. Nazarov, and R.A. Miller, *International Journal of Ion-Mobility Spectrometry* **62** (2001) 15.
29. X. Feng, H.L. Wang, and Y.F. Guan, *Progress in Chemistry* **3** (2005) 514.
30. G.A. Eiceman, D.B. Shoff, C.S. Harden, and A.P. Snyder, *Anal. Chem.* **61** (1989) 1093.
31. "Finland's M90 Detector" *Defence* (Jul 1990) 46.
32. H.H. Hill and G. Simpson, *Field Analytical Chemistry and Technology* **1** 119.
33. H. Paakkanen and J. Huttunen, *Finnish Air Pollut. Prevent. News* **5** (1994) 20.
34. M. Kolehmainen, J. Ruuskanen, E. Rissanen, and O. Raatikainen, *J. of the Air and Waste Manage. Assoc.* **51** (2001) 96.
35. K.Y. Ong, T.L. Longworth, and J.L. Barnhouse, "Domestic Preparedness Program: Testing of M90-D1-C Chemical Warfare Agent Detector Against Chemical Warfare Agents", *U.S. Army Chemical Research and Engineering Center, Aberdeen Proving Ground, MD Summary Report, ECBC-TR-###, UNCLASSIFIED* (Dec 2000).
36. M. Utriainen, "Surveillance and Detection Of C- and B-Agents by Aspiration Ion-Mobility Spectrometry-Based Chemical Detectors", *International Conference on Toxicology ICTX 2004, Tampere, Finland Invited Lecture* (Jul 2004).